Transformation Driven Visual Reasoning

Xin Hong, Yanyan Lan, Liang Pang, Jiafeng Guo, and Xueqi Cheng CAS Key Laboratory of Network Data Science and Technology, Institute of Computing Technology, Chinese Academy of Sciences, Beijing, China University of Chinese Academy of Sciences, Beijing, China

{hongxin19b, lanyanyan, pangliang, guojiafeng, cxq}@ict.ac.cn

Abstract

This paper defines a new visual reasoning paradigm by introducing an important factor, i.e. transformation. The motivation comes from the fact that most existing visual reasoning tasks, such as CLEVR in VQA, are solely defined to test how well the machine understands the concepts and relations within static settings, like one image. We argue that this kind of **state driven visual reasoning** approach has limitations in reflecting whether the machine has the ability to infer the dynamics between different states, which has been shown as important as state-level reasoning for human cognition in Piaget's theory. To tackle this problem, we propose a novel transformation driven visual reasoning task. Given both the initial and final states, the target is to infer the corresponding single-step or multi-step transformation, represented as a triplet (object, attribute, value) or a sequence of triplets, respectively. Following this definition, a new dataset namely TRANCE is constructed on the basis of CLEVR, including three levels of settings, i.e. Basic (single-step transformation), Event (multi-step transformation), and View (multi-step transformation with variant views). Experimental results show that the state-of-the-art visual reasoning models perform well on Basic, but are still far from human-level intelligence on Event and View. We believe the proposed new paradigm will boost the development of machine visual reasoning. More advanced methods and real data need to be investigated in this direction. Code is available at: https://github.com/hughplay/ TVR.

1. Introduction

Visual reasoning is the process of solving problems on the basis of analyzing the visual information, which goes well beyond object recognition [11, 21, 32, 33]. Though the task is easy for humans, it is tremendously difficult for vision systems, because it usually requires higher-order cognition and reasoning about the world. In recent years,

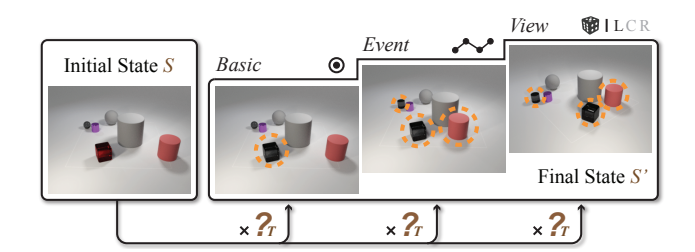


Figure 1. Illustration of three settings in TRANCE. **Basic:** Find the single-step transformation between the initial and final state. **Event:** Find the multi-step transformation between two states. **View:** Similar to Event but the view angle of the final state is randomly chosen from *Left*, *Center* (Default), and *Right*.

several visual reasoning tasks have been proposed and attract a lot of attention in the community of computer vision, machine learning, and artificial intelligence. For example, the most representative visual question answering (VQA) tasks, such as CLEVR [18], define a question answering paradigm to test whether machines have spatial, relational, and other reasoning abilities for a given image. Visual entailment tasks such as NLVR [35, 36] ask models to determine whether a sentence is true about the states of two images. Visual commonsense reasoning tasks, such as VCR [45], further require the model to provide a rationale explaining why its answer is right.

We can see that these visual reasoning tasks are all defined at *state* level. For example, the language descriptions in NLVR and questions answers in VQA and VCR are just related to the concepts or relations within states, i.e. an image, or two images. We argue that this kind of *state driven visual reasoning* definition fails to test the reasoning on dynamics between different states. Take two images as an example. In the first image, there is a cat on a tree, and in the second image, the same cat is under the tree. It is natural for a human to infer that a cat jumps down the tree from the reasoning on the two images. Piaget's cognitive development theory [31] represents the dynamics between

states as transformation, and states that human intelligence must have functions to represent both the transformational and static aspects of reality. In addition, transformation is the key to tackle some more complicated tasks such as storytelling [13] and visual commonsense inference [29]. Though these tasks are closer to reality, they are too complicated to serve as a good testbed for transformation based reasoning. Because many other factors like representation and recognition accuracy may have some effects on the performance. Therefore, it is crucial to define a specific task to test the transformation reasoning ability.

In this paper, we define a novel *transformation driven* visual reasoning (TVR) task. Given the initial and final states, like two images, the goal is to infer the corresponding single-step or multi-step transformation. Without loss of generality, in this paper, transformations indicate changes in object attributes, so a single-step and multi-step transformation are represented as a triplet (object, attribute, value) and a sequence of triplets, respectively.

Following the definition of TVR, we construct a new dataset called TRANCE (TRANSFORMATION ON CLEVR), to test and analyze how well machines can understand transformations. TRANCE is a synthetic dataset based on CLEVR [18], since it is better to first study TVR in a simple setting and then move to more complex real scenarios, just like people first study VOA on CLEVR and then generalize to more complicated settings like GQA. CLEVR has defined five types of attributes, i.e. color, shape, size, material, and position. Therefore, it is convenient to define the transformation for each attribute, e.g. the color of an object is changed from red to blue. Given the initial and final states, i.e. two images, where the final state is obtained by applying a single-step or multi-step transformation on the initial state, a learner is required to well infer such transformation. To facilitate the test for different reasoning levels, we design three settings, i.e. Basic, Event, and View. Basic is designed for testing single-step transformation. Event and View are designed for more complicated multi-step transformation reasoning, where the difference is that View further considers variant views in the final state. Figure 1 gives an example of three different settings.

In the experiments, we would like to test how well existing reasoning techniques [14, 19] work on this new task. However, since these models are mainly designed for existing reasoning tasks, they cannot be directly applied to TRANCE. To tackle this problem, we propose a new encoder-decoder network named TranceNet, specifically for TVR. With TranceNet, existing techniques can be conveniently adapted to TranceNet, by keeping their encoder part unchanged, e.g. ResNet [12], Bilinear-CNN [23] and DUDA [28]. While for the decoder, an adapted GRU [6] network is used to employs the image features and additional provided object attributes by TRANCE to produce

transformation, which is a sequence of triplets. Experimental results show that these models perform well on Basic, but are far from human's level on Event and View, demonstrating high research potentials in this direction.

In summary, the contributions of our work include: 1) the definition of a new visual reasoning paradigm, to learn the dynamics between different states, i.e. transformation; 2) the proposal of a new dataset TRANCE, to test three levels of transformation reasoning, i.e. Basic, Event, and View; 3) experimental studies of the existing SOTA reasoning techniques on TRANCE show the challenges of the TVR and some insights for future model design.

2. Related Works

The most popular visual reasoning task is VQA. Questions in the earliest VQA dataset [2, 10, 46] are usually concerned about the category or attribute of objects. Recent VQA datasets have improved the requirements on image understanding by asking more complex questions, e.g. Visual7W [47], CLEVR [18], OK-VQA [26], and GQA [15]. There are two other forms of visual reasoning tasks that need to be mentioned. Visual entailment tasks, such as NLVR [35, 36], and SNLI-VE [42, 43], ask models to determine whether a given description is true about a visual input. Visual commonsense reasoning [38, 45] tasks require to use commonsense knowledge [37] to answer questions. It is meaningful to solve these tasks which require various reasoning abilities. However, all the above tasks are defined to reason within a single state, which ignore the dynamics between different states.

Recently, several visual reasoning tasks have been proposed to consider more than one state. For example, CATER [9] tests the ability to recognize compositions of object movements. While our target is to evaluate transformations, and our data contains more diverse transformations rather than just moving. Furthermore, CATER along with other video reasoning tasks such as CLEVRER [44] and physical reasoning tasks [3, 4] are usually based on dense states, which make the transformations hard to define and evaluate. Before moving to these complex scenarios, our TVR provides a simpler formulation by explicitely defining the transformations between two states, which is more suitable for testing the ability of transformation reasoning. CLEVR-Change [28] is the most relevant work, which requires a model to caption the changes between two images. However, change caption cannot well define the transformation reasoning, because it ignores some important factors, such as order sensitivity as discussed in the Event setting of Section 4.2.

The concept of transformation has also been mentioned in many other fields. In [16, 22, 27], attribute representations are learned from transformations to improve the classification accuracy. In [1, 8, 25, 39, 48], object or envi-

ronment transformations are detected to improve the performance of action recognition. However, those previous works in attribute learning and action recognition only consider single action, thus not appropriate for testing a complete transformation reasoning ability. Some people may feel that procedure planning [5] has a similar task formulation to TVR and they are closer to reality. However, planning actions in their data are usually very sparse. More importantly, both high-quality recognition and transformation reasoning are crucial to well model the task. As they are coupled together, it is not appropriate to use such tasks to evaluate the transformation reasoning ability. That is why in this paper we use a more simple yet effective way to define the TVR task.

3. The Definition of TVR

TVR (Transformation driven Visual Reasoning) is a visual reasoning task that aims at testing the ability to reason the dynamics between states. Formally, we denote the state and transformation space as S and T respectively. The process of transforming the initial state into the final state can be illustrated as a function $f: \mathcal{S} \times \mathcal{T} \to \mathcal{S}$. Therefore, the task of TVR can be defined as inferring the transformation $T \in \mathcal{T}$ given both the initial state $S \in \mathcal{S}$ and final state $S' \in \mathcal{S}$. The transformation space is usually very large, e.g. any changes of pixel value can be treated as a transformation. Therefore, without loss of generality, we define the atomic transformation as an attribute-level change of an object, represented as a triplet t = (o, a, v), which means the object o with the attribute a is changed to the value v. For example, the color of an object is changed to blue. And further consider the order of atomic transformations, the transformation can be formalized as a sequence of atomic transformations, denotes as $T = \{t_1, t_2, \dots, t_n\}$, where n is the number of atomic transformations.

We make a distinction between the *single-step* (n = 1)and multi-step $(n \ge 1)$ transformation setting because they can be evaluated in different ways to reflect different levels of transformation reasoning abilities. For single-step problems, we can directly compare the prediction T with the ground-truth T to obtain overall accuracy, as well as the fine-grained accuracy of each element in the triplet (o, a, v). With these metrics, it is easy to know how well a learner understands atomic transformations and to analyze the exact reason if the learner performs not well. However, multistep transformation problems cannot be evaluated in this way. Atomic transformations sometimes are independent so that the order of them can be varying, which makes the answer not unique anymore. For example, the order of steps in cooking can not be disrupted but changing the order of cooking different dishes makes no difference to the final result. To tackle the problem, we consider the reconstruction error as the evaluation metric. Specifically, we apply

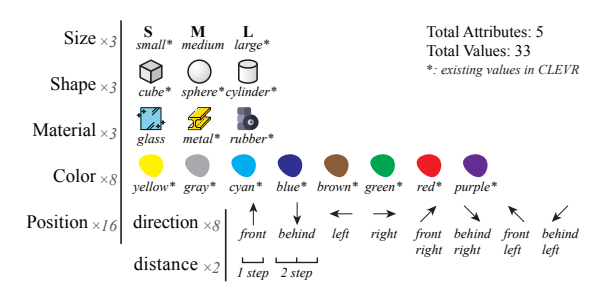


Table 1. Attributes and values in TRANCE.

the predicted transformation \hat{T} to the initial state S, and obtain the predicted final state \hat{S}' . Then we compare the transformed \hat{S}' with the ground-truth final state S' to decide whether the predicted transformation is correct and how far is the distance between the prediction and a correct transformation. Therefore, the evaluation of multi-step problems focuses more on the ability to find all atomic transformations and a feasible order to arrange them.

With this definition, most of the existing state driven visual reasoning tasks can be extended to the corresponding transformation driven ones. For example, the VQA task, such as CLEVR, can be extended to ask the transformation between two given images, with answers as the required transformation. In the extension of NLVR, the task becomes to determine whether a sentence describing the transformation is true about the two images, e.g. the color of the bus is changed to red. Since TVR itself is defined as an interpretation task, we do not need any further rational explanation, and the extension of VCR will stay the same as NLVR. We can see that the essential reasoning target of these tasks is the same, that is to infer the correct transformation. While the difference lies in the manifestation.

4. The TRANCE Dataset

In this paper, we extend CLEVR by asking a uniform question, i.e. what is the transformation between two given images, to test the ability of transformation reasoning. This section introduces how we build the TRANCE (TRANSFORMATION ON CLEVR) dataset following the definition of TVR.

4.1. Dataset Setups

We choose CLEVR [18] to extend, because CLEVR defines multiple object attributes, which can be changed conveniently. With the powerful Blender [7] engine used by CLEVR, we are able to collect over 0.5 million samples with only small computational costs.

According to our definition, an atomic transformation can be represented as a triplet (o, a, v). In the following, we first introduce attribute and value and then object to demonstrate how to ground these factors.

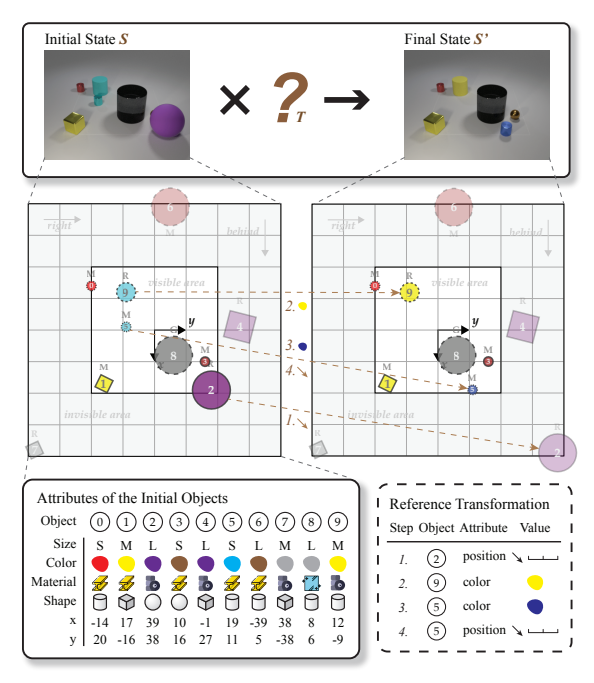


Figure 2. An example from the Event setting.

The setup of the attribute is exactly the same as CLEVR. There are five attributes for each object, i.e. size, color, shape, material, and position.

The value in an atomic transformation is defined corresponding to the concerned attribute, as shown in Table 1. The values of the other four attributes except for position are similar to the default setting of CLEVR. Medium size and glass material are added to enrich the values. The value of position is a little bit complicated since it can be infinite in the space \mathbb{R}^2 . To reduce computation, we replace the absolute value of the position with a relative one. Specifically, two variables, i.e. direction, and step, are used to refer to the target value of a position transformation. We consider eight values for the variable direction, as shown in the Table 1. Then we define a coordinate system, in which x and y are both restricted to [-40, 40]. We require that objects can only be placed on integer coordinates. The variable step can be valued as 1 or 2, where 1 step equals 10 in our coordinate system. Except for normal moving action, we are also interested in whether the vision system could understand actions like moving in and moving out, so the plane is split into the visible area and the invisible area as shown in the middle two images of Figure 2, and the moving in and out operations can be defined correspondingly. To make the transformation process more reasonable, several constraints on the object including no overlapping and no moving out of the plane should be complied with.

The setup for the object is mainly similar to CLEVR. The only problem is how to represent an object in the answer. Existing methods such as CLEVR and CLEVR-

Change [28] use text which is not specific and sometimes results in ambiguity issues when there are two or more similar objects in one image, while CLEVR-Ref+ [24] employs bounding box. In this paper, we propose a method that is specific and easy to evaluate by providing the attributes of the initial objects, as shown in the bottom left of Figure 2, an object can be referred to with the number assigned to it.

To generate data for TRANCE, the first step is the same as CLEVR, which is to randomly sample a scene graph. According to the scene graph, CLEVR then generates questions and answers automatically with a functional program and renders the image with Blender. Different from CLEVR, the next step for TRANCE is to further randomly sample a sequence of atomic transformations $(n \in \{1,2,3,4\})$, which is called as the reference transformation, to transform the initial scene graph to the final scene graph. And the last step is to render two scene graphs into images $(h:240\times w:320)$. The attributes of the initial objects can be easily obtained from the initial scene graph.

To reduce the potential bias in TRANCE, we control the process of scene graph sampling and transformation sampling by considering several factors. In scene graph sampling, we balance the number of visual objects in the initial state and attribute values of objects. In transformation sampling, the length of the transformation, the object number, n-gram atomic transformation, and the move type are all balanced. Throughout all elements, N-gram atomic transformation is the hardest to be balanced and it refers to the sub-sequence of atomic transformations with the length of n. By balancing this factor, we reduce the possibility that a learner utilizes statistics features in the transformation sequences rather than the information from states to predict answers. In the supplementary material, we show the detailed balancing method and the statistics.

4.2. Three Levels of Settings

To facilitate the study on different levels of transformation reasoning, we design three different levels of settings, i.e. Basic, Event, and View. Basic is designed for single-step transformation and Event is designed for multistep transformation. To further evaluate the ability to reason transformation under a more real condition, we extend Event with variant views to propose View. Figure 1 shows an example of three different settings, more examples can be found in the supplementary material.

Basic. Basic is set as the first simple problem to mainly test how well a learner understands atomic transformations. The target of Basic is to infer the single-step transformation between the initial and final states. That is, given a pair of images, the task is to find out which attribute a of which object o has been changed to which value v. We can see that this task is similar to the previous game 'Spot the Difference' [17], in which the player is asked to point out where

are the differences between two images. However, our Basic is essentially different from the game. The game mainly focuses on the pixel level differences between the two images, while Basic focuses on the object level differences. Therefore, Basic can be viewed as a more advanced visual reasoning task than the game.

Event. It is obviously not enough to consider only the single-step transformation. In the real applications, it is very common that multi-step transformation exists between two states. Therefore, we construct this multi-step transformation setting to test whether machines can handle this situation. The number of transformations between the two states is randomly set from 1 to 4. The goal is to predict a sequence of atomic transformations that could reproduce the same final state from the initial state. To resolve this problem, a learner must find all atomic transformations and arrange them with a feasible order. Different from Basic, it is possible to have multiple transformations, which improves the difficulty of finding them all. Meanwhile, the order is essential in the Event setting because atomic transformations may be dependent. For example, in Figure 2, two moving steps, i.e. 1st step and 4th step, cannot be exchanged, otherwise, object 5 and object 2 will overlap.

View The view angle of Basic and Event is uniform, which is not the case in the real applications. To tackle this problem, we extend the Event setting to View, by capturing two states with cameras in different positions. In practice, for simplicity and without loss of generality, we set three fixed cameras, placed in the left, center, and right side of the plane. The initial state is always captured by the center camera, while for the final state, images are captured with all three cameras. Thus, we have three different views of final states for each initial state and obtain three pairs of samples for training, validation, and test. In this way, we are capable to test whether a vision system can understand object-level transformation with variant views.

4.3. Evaluation Metrics

For the single-step transformation setting, i.e. Basic, the answer is unique. Therefore, we can evaluate the performance by directly comparing the prediction with the reference transformation, which is also the ground-truth transformation. Specifically in this paper, we consider two types of accuracy. The first one is fine-grained accuracy corresponds to three elements in transformation triplet, including object accuracy, attribute accuracy, and value accuracy, denoted as *ObjAcc*, *AttrAcc*, and *ValAcc* respectively. The other one is the overall accuracy, which only counts for the absolutely correct transformation triplets, denoted as *Acc*.

For multi-step transformation settings, i.e Event and View, it is not suitable to use the above evaluation metrics, because the answers may not be unique. To tackle this problem, we propose to evaluate the predicted atomic

transformation sequence by checking whether it could reproduce the same final state as the reference transformation. Specifically, we first obtain the predicted final state \hat{S}' by applying the predicted transformation \hat{T} to the initial state S, i.e. $S \times \hat{T} \rightarrow \hat{S}'$. Then a distance is computed by counting the attribute level difference between \hat{S}' and the ground-truth final state S'. To eliminate the influence of different transformation length, we propose to normalize the above distance by the length of the reference transformation to get a normalized distance. Averaging these two metrics on all samples, we obtain AD and AND. We further consider the portion of correct ones, i.e. the distance equals to zero, as the overall accuracy, denoted as Acc. To see whether all atomic transformations are found without considering the order, we omit all constraints such as no overlapping to compute the loose accuracy, which denotes as LAcc. And to measure the ability to assign the right order when all atomic transformations have been found, the error of order EO = (LAcc - Acc)/LAcc is considered. In summary, five evaluation metrics are used in multi-step transformation settings, i.e. AD, AND, LAcc, Acc, and EO.

In the evaluation of multi-step transformation problems, an important step is to obtain the predicted final state \hat{S}' by applying the predicted transformation \hat{T} to the initial state S. This function can be accomplished by our data generation system. However, the whole generation process includes image rendering which is time-consuming. Therefore, we extract the core function that transforms the initial scene graph to the final graph, to construct a fast evaluation system for multi-step transformation evaluation. Except for the usage of evaluation, this newly constructed evaluation system can also be used to generate reward signals for reinforcement learning, which is explored in Section 5.2.

5. Experiments

In this section, we show our experimental results on the three settings of TRANCE, i.e. Basic, Event, and View. We also conduct some analyses of the results to show insights about machines' ability to reason transformation.

5.1. Models

Firstly, we would like to test how well existing methods will work on this new task. However, since the inputs and outputs of TVR are quite different from existing visual reasoning tasks, existing methods like [14, 19] cannot be directly applied. So we design a new encoder-decoder style framework named TranceNet. As Figure 3 shows, the encoder first extracts features from input image pairs, and then a GRU based decoder is employed to generate transformation sequences. The following of this section briefly introduces our TranceNet framework while the implementation details can be found in the supplementary material. To compare with humans, for each of the three settings, we

also collect results of 100 samples in total. These results come from 10 CS Ph.D. candidates who are familiar with the problems and our testing system.

Encoder. The encoder is to extract effective features from image pairs, which are mainly associated with the difference between the two states. To extract these features, there are two ways can be employed, namely single-stream way or two-stream way, either by directly inputting two images into a network to encode or first extracting image features separately and then find the difference in the feature space. In this paper, we set six methods falling into these two categories. For the single-stream way, we test two networks, i.e. Vanilla CNN and ResNet [12], combined with two preprocessing techniques, i.e. subtraction (–) and concatenation (⊕). For example, we use ResNet_⊕ to represent a ResNet fed with concatenated image pairs. Another two methods are Bilinear CNN (BCNN [23]) and a recent method called **DUDA** [28], which operate as the two-stream way. BCNN is a classical model for fine-grained image classification to distinguish categories with small visual differences. DUDA is originally proposed for change detection and captioning. The main difference between BCNN and DUDA lies in the way of feature-level interaction.

Decoder. The decoder is used to output a feasible transformation sequence from extracted image features. We adopt a uniform GRU [6] network for all six encoders, which is commonly used in sequence generation. As shown in Figure 3, the major difference between our GRU network and an ordinary one lies in the additional classifier. The classifier accepts attributes of the initial objects and the current hidden state from the GRU cell, and then outputs object and value for the atomic transformation of the current step. In detail, an object vector is first computed from the hidden state. Then the object of the current atomic transformation is obtained by matching the object vector with the initial objects using cosine similarity. Finally, the most similar object vector from initial objects and the hidden state are used to predict the value of the current atomic transformation. In TRANCE, attributes are implied by values, for example, blue indicates that the attribute is color, so that the output of a classifier does not explicitly include an attribute.

Since all these models share the same decoder, we will denote these models by their encoders' names hereafter.

Training. The loss function of a single sample consists of two cross-entropy losses, i.e. object loss and value loss, which can be represented as:

$$\mathcal{L}(T,\hat{T}) = -\frac{1}{n} \sum_{i=1}^{n} (t_i^o \cdot \log \hat{t}_i^o + t_i^v \cdot \log \hat{t}_i^v), \qquad (1)$$

where n is the transformation length of the evaluation sample, t_i^o and t_i^v denote the object and value at the i-th step transformation. The training loss is the average of losses over all training examples. During training, we use teacher

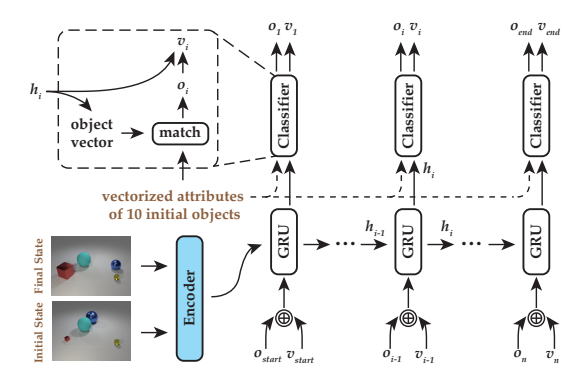


Figure 3. The architecture of TranceNet.

forcing [41] for faster convergence in TranceNet. Firstly, we follow the practice in sequence learning such as machine translation, to use the object and value from the given reference transformation as inputs in each step of GRU. Additionally, objects from reference transformations are used to predict values in the classifier.

5.2. Results on Three Settings

In this section, we first present our experimental results on the three settings of TRANCE, and then provide some in-depth analyses on the results.

We test six models in the Basic setting of TRANCE, i.e. CNN_- , CNN_\oplus , $ResNet_-$, $ResNet_\oplus$, BCNN, DUDA. From the results in the left part of Table 2, we can see that all models perform quite well, in the sense that the performance gap between these models and humans is not very large. Comparing these models, both versions of ResNet perform better than BCNN and DUDA. As we mentioned before, CNN and ResNet are single-stream methods while BCNN and DUDA are two-stream methods. Since the model size of ResNet, BCNN, and DUDA is similar, we can conclude that the single-stream way is better than the two-stream way on the Basic setting. Further checking the fine-grained accuracy, we can see this gap comes from the ability to find the correct object and value, while all models are good at distinguishing different attributes.

The experimental results on Event are shown in the middle part of Table 2. We can see that this task is very challenging for machines, since there is an extremely big performance gap between models and human. That is because the answer space rises exponentially when the number of steps increases. In our experiments, the size of answer space is $\sum_{i=1}^4 (33\times 10)^i$, about 11.86 billion. The performance (e.g. Acc) gap between CNN and ResNet models becomes larger from Basic to Event, which suggests large encoders have advantages in extracting sufficient features to decode transformation sequences.

We also employ reinforcement learning to train our model. Specifically, the evaluation system introduced in

Model	Basic			Event			View					
1.10 301	ObjAcc	AttrAcc	ValAcc	Acc	AD	AND	LAcc	Acc	AD	AND	LAcc	Acc
CNN_	0.9584	0.9872	0.9666	0.9380	1.5475	0.5070	0.4587	0.4442	2.2376	0.8711	0.2344	0.2286
CNN_{\oplus}	0.9581	0.9889	0.9725	0.9420	1.4201	0.4658	0.4981	0.4838	2.2517	0.8764	0.2350	0.2285
$ResNet_{-}$	0.9830	0.9969	0.9935	0.9796	1.0974	0.3417	0.5972	0.5750	1.1068	0.3749	0.5484	0.5272
$ResNet_{\oplus}$	0.9852	0.9980	0.9928	0.9810	1.0958	0.3469	0.6019	0.5785	1.1148	0.3731	0.5525	0.5305
BCNN	0.9705	0.9950	0.9788	0.9571	1.1081	0.3582	0.5746	0.5560	1.2633	0.4395	0.4977	0.4784
DUDA	0.9453	0.9888	0.9692	0.9320	1.5261	0.4975	0.5025	0.4856	1.5352	0.5242	0.4746	0.4590
Human	1.0000	1.0000	1.0000	1.0000	0.3700	0.1200	0.8300	0.8300	0.3200	0.0986	0.8433	0.8433

Table 2. Model and human performance on Basic, Event, and View.

Model	AD	AND	LAcc	Acc
ResNet⊕	1.0958	0.3469	0.6019	0.5785
+ corr	1.0579	0.3316	0.6215	0.5978
+ dist	1.0528	0.3319	0.6180	0.5938
+ corr & dist	1.0380	0.3251	0.6230	0.6001

Table 3. Results of ResNet $_{\oplus}$ trained using REINFORCE [40] with different rewards on Event.

Section 4.3 is able to provide signals include the *correctness* of a prediction and the *distance* between a prediction and one of the correct transformations. These signals could be used as rewards in REINFORCE [40] algorithm to further train a ResNet $_{\oplus}$ model. Table 3 shows that training with three different rewards will significantly improve the performance, and the difference among these rewards is small.

The right part of Table 2 shows the results on the View setting. While humans are insensitive to view variations, the performances of all the above models drop sharply from Event to View. Among these models, the most robust one is DUDA. From the fact that a similar two-stream architecture is used in BCNN but performs worse, we can see that the methods of directly interacting two state features in DUDA play an important role in tackling the view variation.

5.3. Detailed Analysis on Event and View

According to the above experimental results, the performances on Event and View are not good. So we conduct some detailed analysis of these data, to help understand the tasks and provide some insights for future model design.

Firstly, we analyze the effect of transformation sequence length on Event, which is the main factor to make models perform worse as compared with Basic. Specifically, we categorize all the test samples into four kinds, based on their lengths, i.e. samples with k-step transformation, k=1,2,3,4. Then we plot the LAcc for each group in Figure 4. From the results, we can see that both humans and the deep learning models work quite well when the length is short, e.g. 1. As the length increases, humans still have the ability to well

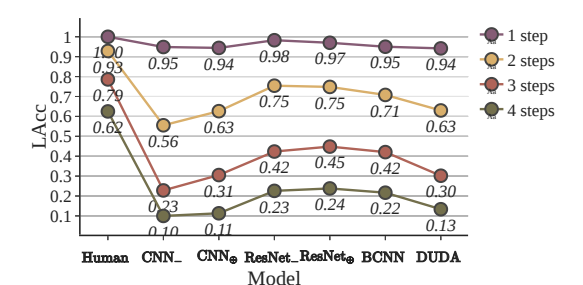


Figure 4. Results on Event with respect to different steps.

Encoder	LAcc	Acc	ЕО
Random (avg. of 100)	1.0000	0.4992	0.5008
CNN_	0.2276	0.2067	0.0915
CNN_{\oplus}	0.2596	0.2244	0.1358
$ResNet_{-}$	0.3478	0.2997	0.1382
$ResNet_{\oplus}$	0.3862	0.3205	0.1701
BCNN	0.2949	0.2612	0.1141
DUDA	0.2500	0.2147	0.1410
Human	0.7273	0.7273	0.0000

Table 4. Results of order sensitive samples on Event (7.8%).

capture the complicated transformations, however, the current deep learning models decline sharply. Take CNN_{-} as an example, the performances for the four different groups are 95%, 56%, 23%, and 10%. These results indicate that future studies should focus more on how to tackle transformations with long steps.

Then we analyze the effect of orders on Event, which is another important factor in this data. According to our statistics, for 7.8% test samples¹, there exists some permutation that violates our constraints such as no overlapping. That is to say, these samples are order sensitive. Even if the algorithm finds all correct atomic transformations, it will still make some mistakes without carefully considering the order among these transformations. Table 4 shows the re-

¹We have also tried other data with different percentages, e.g. 25%, and the results are similar.

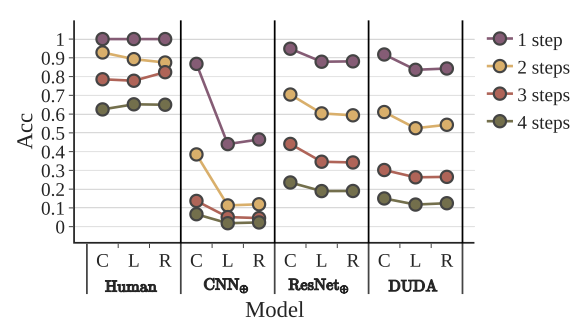


Figure 5. Results for different final views (Center, Left, Right).

sults on these order sensitive samples, where EO is directly defined to measure the influence of order, LAcc and Acc are just listed for reference. From the results, we can see that EO for the human is zero. Therefore, once humans find all correct transformations, they are easy to figure out the orders. However, for all the models, the EO values are larger than zero, which indicates a clear effect of the order on the reasoning process. In order to find out how large is the effect, i.e., whether $0.0915 \sim 0.1701$ means a large deviation, we perform 100 random experiments. Specifically in each run, we randomly assign a transformation order to each order sensitive test sample. As a result, the averaged EO value is 0.5008, which could be viewed as an upper bound of an order error. Therefore, the current deep learning models have some ability to tackle the orders, but there is still some room for improvements.

At last, we analyze the effect of view variation. For each model, we separate the results of different views, as shown in Figure 5. Please note that the results of CNN_, ResNet_, and BCNN are quite similar to CNN⊕, ResNet⊕ and DUDA, so we just give three representative results. Firstly, humans' results across different views are almost the same, demonstrating human's high ability to adapt to different views. In some cases, humans' performances in terms of view variations are even better than the case that views are unchanged. That is because when the view changes, humans usually spend more time on that, which makes the performance higher. For the deep learning models, they show a similar trend that view variations will hurt the performance. Among them, CNN models decrease the most, while DUDA is the most robust one. These results show that models with more parameters are more robust to view variations. Besides, feature-based interactions, like the way used in DUDA, is helpful. Nevertheless, there is still a gap between the current models and the human, which needs to be considered in future model design.

5.4. Analysis of Training Data Size

In our experiments, we find that data size is an important factor for training and evaluation. So we use $ResNet_{\oplus}$ as an example to show the influences of different data sizes in

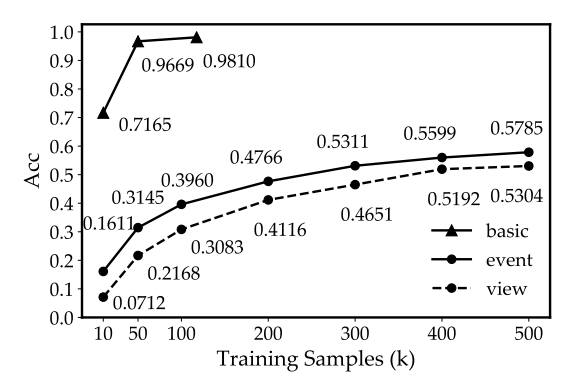


Figure 6. Results of ResNet \oplus with different training size.

Figure 6. From this figure, we can see that more data brings significant benefits when the training samples are less than 50k on Basic and 200k on Event and View. After that, the benefit becomes smaller and smaller. Those results are consistent with the general understanding that a relatively large data is required to well train a deep learning model. These results also show that the current data size of TRANCE is sufficient in our experiments.

6. Conclusion

To tackle the problem that most existing visual reasoning tasks are defined on static settings and cannot well capture the dynamics between states, we propose a new visual reasoning paradigm, namely transformation driven visual reasoning (TVR). Given the initial and final states, the target is to infer the corresponding single-step transformation or multi-step transformations, represented by a triplet (object, attribute, value) or a sequence of triplets, respectively. In this paper, we use CLEVR as an example, to construct a new synthetic data, namely TRANCE, which includes three different levels of setting, i.e. Basic for single-step transformation, Event for multi-step transformations, and View for multi-step transformation with variant views. To study the effectiveness of existing SOTA reasoning techniques, we propose a new encoder-decoder framework named TranceNet, which includes six different encoder models such as ResNet, Bilinear-CNN, and DUDA. The experimental results show that these models work well on Basic, while still have difficulties in Event and View. Specifically, the major difficulties for Event come from finding all atomic transformations and a feasible order to arrange them when the length of the transformation sequence is large. While for View, the view variations bring great challenges to these models, but effect litter on the human.

In the future, we plan to conduct investigations from both model and data perspectives, including testing other methods such as neural symbolic approach, and constructing real dataset to study TVR.

Supplementary Material

Following sections aim at providing additional materials to supplement our main submission. We first show the detail of data balancing on TRANCE in Section A. Then, we give more details on the implementation of the baseline models and training in Section B. Next in Section C, we describe the test system we used for collecting results from humans. Finally in Section D, we provide extra examples of three settings from TRANCE, i.e. Basic, Event, and View.

A. Dataset Balance

Data balancing is an important factor to be considered when constructing TRANCE. Several factors are balanced in TRANCE, so that a learner is expected to reason the transformation without utilizing the biased features such as the length of transformation in data. Without considering the image rendering, the data generation process consists of two stages, i.e. sampling an initial scene graph and sampling a transformation sequence to transform the initial scene graph into the final scene graph. In the following of this section, we first introduce the factors that are balanced in these two stages and then describe the method we used.

When sampling the initial scene graph, the number of visual objects and the attribute values of all objects are balanced strictly. Recall that the plane is separated into the visible area and invisible area and only objects in the visible area appear in the image of the initial state. The two diagrams on the top row of Figure 7 show the statistics of these two factors.

When sampling the transformation sequence, we balance four factors in total. The first factor is the length of transformation so that the numbers of samples with different transformation lengths are equal. The statistic result of the transformation length can be found on the left of the second row in Figure 7. The other three factors target to the elements of atomic transformations. For the part of object, we balance the object number, and for the value, we balance the n-gram atomic transformation and the move type. The object number is directly balanced over all samples and the result is shown in the middle of the second row in Figure 7. As for the value, it should be handled more carefully than the object number, since for a specific initial scene graph, the availability of different atomic transformations is different. For example, changing the color of one object can always be successful, but changing the position of an object with a specific direction and step may be failed because of overlapping. Furthermore, without considering to balance the value throughout the sub-sequence of atomic transformations, the possibility of the concurrence of atomic transformations with low successful probability will be much lower than others. For example, four atomic transformations on position will be less possible than four atomic transformations on color exist in one sequence. We called sub-sequence with the length n as n-gram atomic transformations. Table 5 shows the statistics of this factor. For each n-gram, the number of different options to be chosen is shown in the first row. For example, we have 33 different values so that the options of 1-gram are 33 and that of 2-gram is $33^2 = 1089$ and so on. We count the n-gram options with different sizes of sliding windows on all sampled transformation sequences. For example, we use a 2-length sliding window with 1 stride to count 2-gram atomic transformations on a 4-step transformation. Therefore, a 4-step contains three 2-gram atomic transformations. The remaining rows of Table 5 are calculated on the counting results of options under each n-gram. From the table, the standard variance is very small compared to the mean value, which means the samples of different options under a specific ngram is nearly equal. However, the size of TRANCE is 0.5 million, which is not enough to cover all 4-gram options, but the analysis of training data size has proved our data is sufficient for training a deep model. In conclusion, the ngram atomic transformation is carefully balanced to eliminate the negative effect caused by the different availability of different atomic transformations. Additionally, we balance the move type over all samples and the result is shown in the right of the second row in Figure 7.

The method we used to balance all the above factors is balanced sampling. The basic idea of this method is changing the sampling probability dynamically according to previously generated samples. Algorithm 1 shows how to sample an option from all available alternatives given the count table of previously generated all options.

B. Implementation Details

The code for data generation is rewritten on the basis of the original code of CLEVR². As for training, we use PyTorch [30] as our deep learning framework. In the following, we introduce the implementation of our baseline models and training process in detail.

Table 6 shows the constitution of different baseline models under the TranceNet framework. In the encoder part, both CNN_{-} and CNN_{\oplus} use a 4-layer CNN as the backbone of the encoder. The channel of four CNN layers is 16, 32, 32, 64, the kernel size is 5, 3, 3, and all the strides is 2. The encoder backbone of $ResNet_{-}$, $ResNet_{\oplus}$, and DUDA is $ResNet_{-}18$ [12], which we directly use the implementation given by PyTorch without pretrained parameters. As for BCNN, we use the VGG-18 [34] implemented by PyTorch as the backbone of the encoder, which is consistent with the original paper [23]. In the decoder part, the output of the encoder is first flattened and then encoded by a fully-connected layer to be a 128-dimension vector. This

²https://github.com/facebookresearch/clevr-dataset-gen

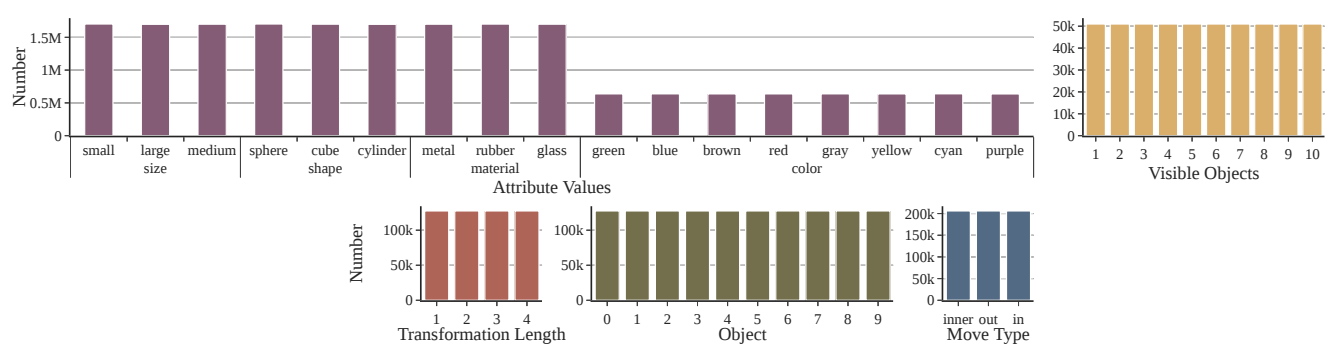


Figure 7. The statistics of balanced factors in the TRANCE dataset. **Top Row:** attribute values and visible objects during sampling the initial scene graphs. **Bottom Row:** transformation length, object number, and move type during sampling transformation sequences.

	1-gram	2-gram	3-gram	4-gram
options	33	1,089	35,937	1,185,921
min	38,635	697	7	0
max	38,638	708	15	3
median	38,636	703	11	0
mean	38,636	702.5	10.64	0.1075
std	0.7714	2.2854	0.7880	0.3150

Table 5. The statistics of the n-gram atomic transformations in TRANCE.

Algorithm 1: Balanced Sampling					
Input: available k options $O = \{o_1, o_2,, o_k\},\$					
corresponding count table					
$N = \{n_1, n_2,, n_k\};$					
Output: sampled option o_r ;					
Parameter: tolerance $t = 0.1$ (default);					
$n_{max} = \max(n_1, n_2,, n_k);$					
$c_i = n_{max} - n_i + t ;$					
$\mathfrak{z} p_i = \frac{c_i}{\sum_{i=1}^k c_i} ;$					
4 o_r = randomly sample an option from					
$\{o_1, o_2,, o_k\}$ with probability $\{p_1, p_2,, p_k\}$;					

128-dimension vector will be sent to the adapted GRU network. In each cell of the adapted GRU network, the hidden size of the GRU cell is 128 and two 1-layer fully-connected layers are used to decode the object vector and the value of each step respectively. The dimension of the object vector is 19, 8 for the color, 3 for the size, 3 for the shape, 3 for the material, and 2 for the position. The dimension of the value output is 33.

The optimizer used for training is Adam [20]. The learning rate used by Adam is 0.001 in the beginning and is reduced to 0.0001 after 25 epochs. For the settings of Event and View, data is shared and the size of the training, validation, test set is 500,000, 2,000, and 8,000 respectively. For the setting of Basic, we collect all existing 1-step sam-

Model	Encoder Backbone	Decoder	Parameters
CNN_	4-layer CNN	Adapted GRU	737K
CNN_{\oplus}	4-layer CNN	Adapted GRU	738K
$ResNet_{-}$	resnet18	Adapted GRU	11M
$ResNet_{\oplus}$	resnet18	Adapted GRU	11M
BCNN	vgg11_bn	Adapted GRU	41M
DUDA	resnet18	Adapted GRU	18M

Table 6. Different baseline models under the TranceNet framework.

ples in data, and the size of training, validation, and test set is 117,500, 2,000, and 8,000. All models are trained with 50 epochs on the training set and models that have the best results on the validation set are chosen to be evaluated on the test set to get the final results. In our experiments, images are resized to 120×160 for fast training. Furthermore, by following the common practice on image augmentation [21], we apply a $0 \sim 5\%$ spatial translation to input image pairs during the training process.

C. Human Test System

To collect results from the human, we build a web-based test system. Figure 8 shows the GUI of this system. The whole testing process is described as the following steps. First of all, a human tester is told to be familiar with the system by trying a few examples with guidance. After that, the tester changes the user name and the target problem to start testing. During the testing of each sample, the tester should select the correct atomic transformations arranged with a feasible order after observing the initial, the final state, and the attributes of the initial objects. To reduce the time usage, we also provide the visualization of the initial objects for testers. After that, the tester can submit the answer and start to answer the next sample. After completing all test samples, the tester can see his or her test result by clicking the button under the testing history. The code for the human test system is also publicly available.

D. More Examples from TRANCE

The remaining pages show extra examples from the three settings of TRANCE, i.e. Basic, Event, and View. In each sample, the initial state, the final state, and the attributes of the initial objects are given. In the View setting, the view angle of the final state is only randomly selected from Left and Right, since samples with the Center view is similar to the samples from the Event setting. Besides, for each sample, an additional diagram is provided to visualize the attributes of the initial objects. At last, we show the reference transformation.

When moving an object from the visible area into the invisible area, any directions and steps that could cause the same effect without making objects overlapping are accepted. This is implemented by only comparing the visible objects' attribute values of the final states in the evaluation system.

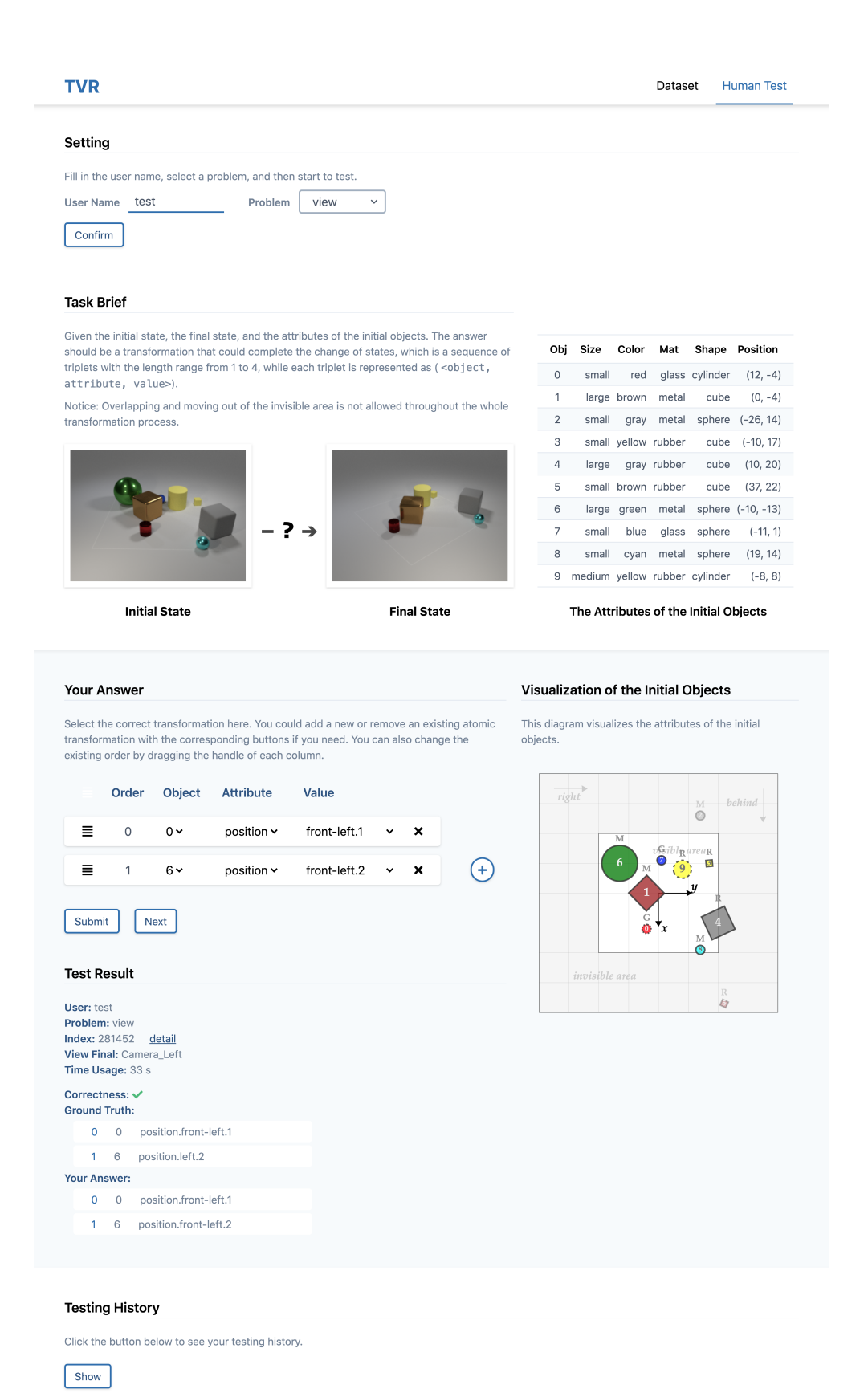


Figure 8. Human test system.

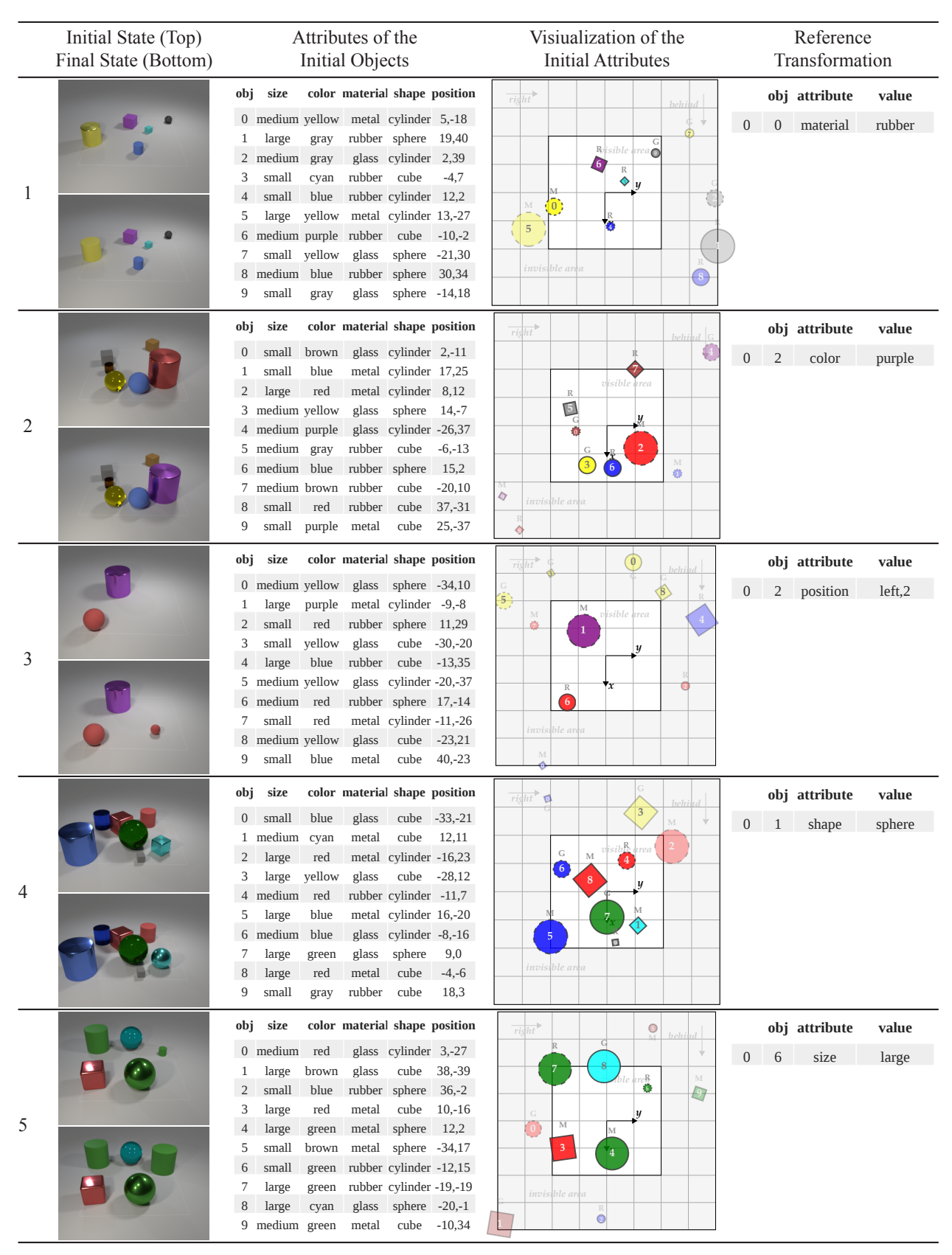


Figure 9. Examples from the Basic setting.

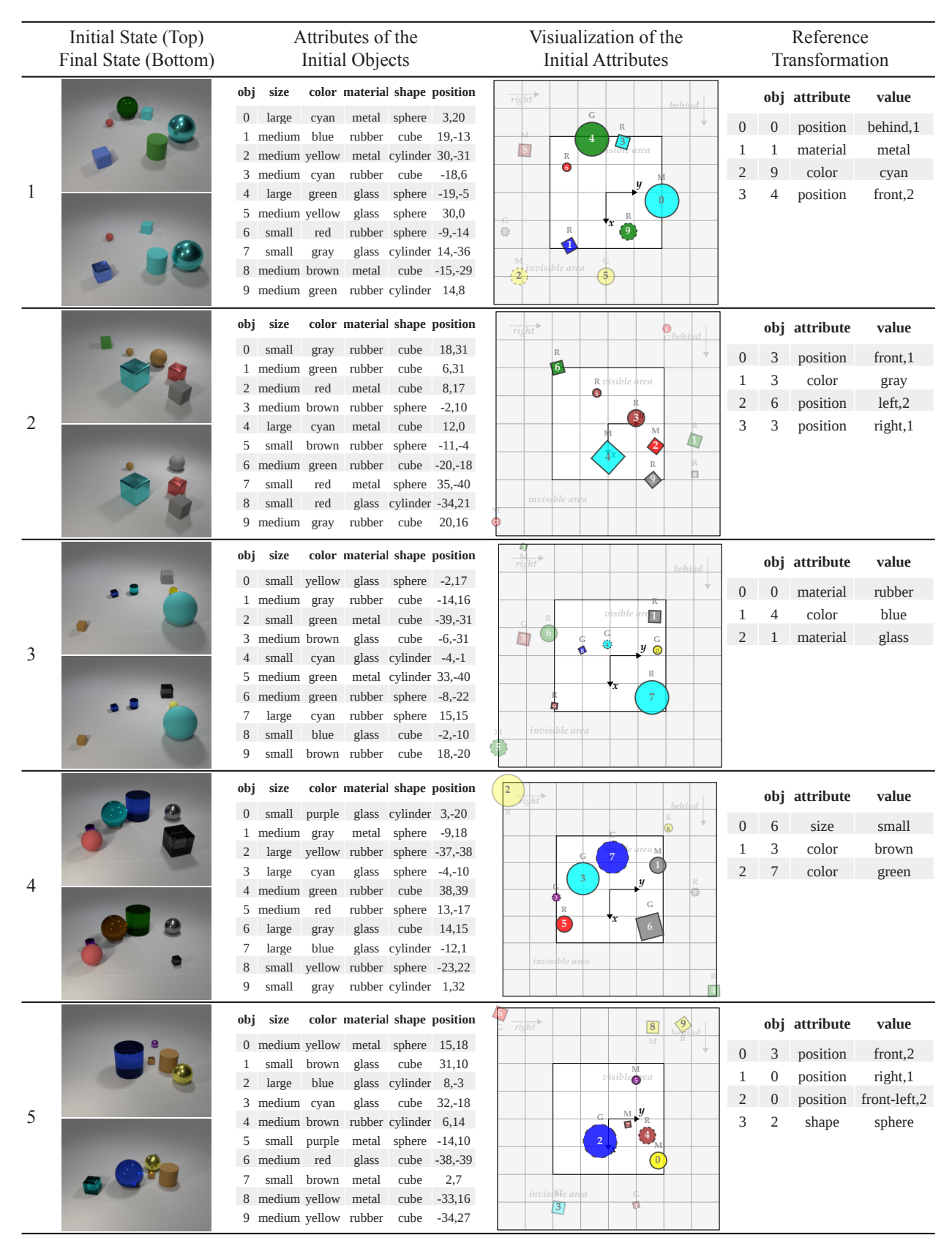


Figure 10. Examples from the Event setting.

	Initial State (Top) Final State (Bottom)	Attributes of the Initial Objects	Visiualization of the Initial Attributes	Reference Transformation
		obj size color material shape position	right behind	obj attribute value
		0 small red rubber cube 16,-20 1 medium red rubber cylinder -6,17	M R	0 5 position front,1
		2 small green glass sphere 2,19	wisible at 4	1 5 color cyan
		3 small gray rubber cube 24,23	S	2 0 size medium
1		4 large blue rubber cube -18,16		3 1 position right,2
		5 large red metal cylinder 20,-4	R M X	
		6 small green metal sphere -8,-29	G B R	
		7 small red metal cylinder -20,-8	nivisible area	
		8 medium blue metal cube 2,-30 9 large blue glass cube 23,-31		
		5 large blue glass cube 25, 51		
		obj size color material shape position	right ▶ hchivd	obj attribute value
		0 small yellow metal cylinder 21,-38	M R	0 5 position behind-left,2
		1 large yellow rubber cube -4,1	R R R R	1 1 color green
		2 large green metal sphere -9,20	2	2 2 size medium
2		3 medium purple rubber sphere 38,-21	7 6 1 y	3 2 position front-left,1
_		4 medium red rubber cylinder 13,-11 5 medium blue rubber sphere 12,9	R	P
	- B- A	6 large green rubber cube -3,-14	M 4x 5	
		7 large blue rubber sphere -3,-31	: <u>0</u> :	
		8 medium green metal sphere -21,-16	invisible area	
		9 small cyan rubber cylinder -23,-7	3	
		obj size color material shape position	right M behind G	ahi attributa saha
			right hehind 0	obj attribute value
		0 medium brown glass sphere -29,38 1 medium cyan glass cube -17,14	M G	0 8 material rubber
		2 large gray metal cylinder -27,-11	6 visible a	1 4 size small
		3 small purple glass cylinder 13,19	M R	2 5 shape cylinder
3		4 medium purple rubber cube 20,-13	5	
	- 1	5 large red rubber cube 0,16	x G	
		6 medium gray metal cylinder -15,-5	R 4	
		7 small blue glass cylinder 27,37	invisible area	
		8 small green metal sphere -6,3 9 small blue rubber cylinder 38,12	R	
		- Januar State Tubber Cymiaer 30,12		
		obj size color material shape position	right G habited	obj attribute value
		0 medium cyan glass cube 32,21	M A	0 4 position behind,1
		1 large blue rubber cube 11,-1	Vible grea	1 5 size medium
		2 medium green metal sphere 17,-27	9 M	2 7 shape cube
4		3 large blue metal cylinder -22,-29 4 medium green glass cube -27,13	M	3 7 material glass
•		4 medium green glass cube -27,13 5 large red metal cube 1,16	8 R	5 / material glass
	<u> </u>	6 medium brown glass cylinder 7,-38	M 11V	
		7 medium purple metal sphere -20,-16		
		8 medium cyan metal sphere 3,-15	invis ble area	
		9 large cyan metal cube -8,1		
		obj size color material shape position	3.4 Palaind	obj attribute value
5		0 medium red rubber sphere -14,-1	3 behind	_
		1 small green metal cube 12,-1	R	0 4 position right,2
		2 small gray glass sphere -34,9	0 9	1 9 material metal
		3 large cyan glass cube -33,-32	y	2 9 color gray
		4 medium blue glass cube 15,-10		
		5 small yellow rubber cylinder -29,20	Mx	
		6 small blue metal sphere 36,29 7 medium purple glass cube 16,21		
	9.	8 medium cyan metal sphere 28,-36	M (8) invisible area	
		9 large purple rubber cylinder -17,10	M	
		. O. r. r		

Figure 11. Examples from the View setting.

References

- [1] Jean-Baptiste Alayrac, Ivan Laptev, Josef Sivic, and Simon Lacoste-Julien. Joint discovery of object states and manipulation actions. In *Proceedings of the IEEE International Conference on Computer Vision*, pages 2127–2136, 2017. 2
- [2] Stanislaw Antol, Aishwarya Agrawal, Jiasen Lu, Margaret Mitchell, Dhruv Batra, C. Lawrence Zitnick, and Devi Parikh. VQA: Visual Question Answering. In *International Conference on Computer Vision (ICCV)*, 2015.
- [3] Anton Bakhtin, Laurens van der Maaten, Justin Johnson, Laura Gustafson, and Ross Girshick. Phyre: A new benchmark for physical reasoning. In Advances in Neural Information Processing Systems, pages 5082–5093, 2019. 2
- [4] Fabien Baradel, Natalia Neverova, Julien Mille, Greg Mori, and Christian Wolf. Cophy: Counterfactual learning of physical dynamics. In *ICLR*, 2020. 2
- [5] Chien-Yi Chang, De-An Huang, Danfei Xu, Ehsan Adeli, Li Fei-Fei, and Juan Carlos Niebles. Procedure planning in instructional videos. arXiv preprint arXiv:1907.01172, 2019.
- [6] Kyunghyun Cho, Bart van Merriënboer, Caglar Gulcehre, Dzmitry Bahdanau, Fethi Bougares, Holger Schwenk, and Yoshua Bengio. Learning phrase representations using rnn encoder-decoder for statistical machine translation. In Proceedings of the 2014 Conference on Empirical Methods in Natural Language Processing (EMNLP), pages 1724–1734, 2014. 2, 6
- [7] Blender Online Community. Blender–a 3d modelling and rendering package, 2016. 3
- [8] Alireza Fathi and James M Rehg. Modeling actions through state changes. In *Proceedings of the IEEE Conference* on Computer Vision and Pattern Recognition, pages 2579– 2586, 2013. 2
- [9] Rohit Girdhar and Deva Ramanan. CATER: A diagnostic dataset for Compositional Actions and TEmporal Reasoning. In *ICLR*, 2020. 2
- [10] Yash Goyal, Tejas Khot, Douglas Summers-Stay, Dhruv Batra, and Devi Parikh. Making the V in VQA matter: Elevating the role of image understanding in Visual Question Answering. In *Proceedings of the IEEE Conference on Computer Vision and Pattern Recognition*, pages 6904–6913, 2017. 2
- [11] Kaiming He, Georgia Gkioxari, Piotr Dollár, and Ross Girshick. Mask r-cnn. In *Proceedings of the IEEE international conference on computer vision*, pages 2961–2969, 2017. 1
- [12] Kaiming He, Xiangyu Zhang, Shaoqing Ren, and Jian Sun. Deep residual learning for image recognition. In *Proceedings of the IEEE conference on computer vision and pattern recognition*, pages 770–778, 2016. 2, 6, 9
- [13] Ting-Hao Huang, Francis Ferraro, Nasrin Mostafazadeh, Ishan Misra, Aishwarya Agrawal, Jacob Devlin, Ross Girshick, Xiaodong He, Pushmeet Kohli, Dhruv Batra, et al. Visual storytelling. In Proceedings of the 2016 Conference of the North American Chapter of the Association for Computational Linguistics: Human Language Technologies, pages 1233–1239, 2016.
- [14] Drew A Hudson and Christopher D Manning. Compositional attention networks for machine reasoning. arXiv preprint arXiv:1803.03067, 2018. 2, 5

- [15] Drew A. Hudson and Christopher D. Manning. GQA: A new dataset for real-world visual reasoning and compositional question answering. In *The IEEE Conference on Computer Vision and Pattern Recognition (CVPR)*, June 2019. 2
- [16] Phillip Isola, Joseph J Lim, and Edward H Adelson. Discovering states and transformations in image collections. In Proceedings of the IEEE conference on computer vision and pattern recognition, pages 1383–1391, 2015.
- [17] Jung-Hwan Jin, Hyun Joon Shin, and Jung-Ju Choi. Spoid: a system to produce spot-the-difference puzzle images with difficulty. *The Visual Computer*, 29(6-8):481–489, 2013. 4
- [18] Justin Johnson, Bharath Hariharan, Laurens van der Maaten, Li Fei-Fei, C Lawrence Zitnick, and Ross Girshick. CLEVR: A diagnostic dataset for compositional language and elementary visual reasoning. In CVPR, 2017. 1, 2, 3
- [19] Justin Johnson, Bharath Hariharan, Laurens Van Der Maaten, Judy Hoffman, Li Fei-Fei, C Lawrence Zitnick, and Ross Girshick. Inferring and executing programs for visual reasoning. In *Proceedings of the IEEE International* Conference on Computer Vision, pages 2989–2998, 2017. 2, 5
- [20] Diederik P. Kingma and Jimmy Ba. Adam: A method for stochastic optimization. In Yoshua Bengio and Yann LeCun, editors, 3rd International Conference on Learning Representations, ICLR 2015, San Diego, CA, USA, May 7-9, 2015, Conference Track Proceedings, 2015. 10
- [21] Alex Krizhevsky, Ilya Sutskever, and Geoffrey E Hinton. Imagenet classification with deep convolutional neural networks. In Advances in neural information processing systems, pages 1097–1105, 2012. 1, 10
- [22] Yong-Lu Li, Yue Xu, Xiaohan Mao, and Cewu Lu. Symmetry and group in attribute-object compositions. In *Proceedings of the IEEE/CVF Conference on Computer Vision and Pattern Recognition*, pages 11316–11325, 2020. 2
- [23] Tsung-Yu Lin, Aruni RoyChowdhury, and Subhransu Maji. Bilinear CNN models for fine-grained visual recognition. In Proceedings of the IEEE international conference on computer vision, pages 1449–1457, 2015. 2, 6, 9
- [24] Runtao Liu, Chenxi Liu, Yutong Bai, and Alan L Yuille. CLEVR-Ref+: Diagnosing visual reasoning with referring expressions. In Proceedings of the IEEE Conference on Computer Vision and Pattern Recognition, pages 4185– 4194, 2019. 4
- [25] Yang Liu, Ping Wei, and Song-Chun Zhu. Jointly recognizing object fluents and tasks in egocentric videos. In Proceedings of the IEEE International Conference on Computer Vision, pages 2924–2932, 2017.
- [26] Kenneth Marino, Mohammad Rastegari, Ali Farhadi, and Roozbeh Mottaghi. OK-VQA: A visual question answering benchmark requiring external knowledge. In *Proceed*ings of the IEEE Conference on Computer Vision and Pattern Recognition, pages 3195–3204, 2019. 2
- [27] Tushar Nagarajan and Kristen Grauman. Attributes as operators: factorizing unseen attribute-object compositions. In *Proceedings of the European Conference on Computer Vision (ECCV)*, pages 169–185, 2018. 2
- [28] Dong Huk Park, Trevor Darrell, and Anna Rohrbach. Robust change captioning. In *The IEEE International Conference on Computer Vision (ICCV)*, October 2019. 2, 4, 6

- [29] Jae Sung Park, Chandra Bhagavatula, Roozbeh Mottaghi, Ali Farhadi, and Yejin Choi. Visualcomet: Reasoning about the dynamic context of a still image. In *In Proceedings of the European Conference on Computer Vision (ECCV)*, 2020. 2
- [30] Adam Paszke, Sam Gross, Francisco Massa, Adam Lerer, James Bradbury, Gregory Chanan, Trevor Killeen, Zeming Lin, Natalia Gimelshein, Luca Antiga, Alban Desmaison, Andreas Kopf, Edward Yang, Zachary DeVito, Martin Raison, Alykhan Tejani, Sasank Chilamkurthy, Benoit Steiner, Lu Fang, Junjie Bai, and Soumith Chintala. Pytorch: An imperative style, high-performance deep learning library. In Advances in Neural Information Processing Systems 32, pages 8024–8035. Curran Associates, Inc., 2019. 9
- [31] Jean Piaget. The role of action in the development of thinking. In *Knowledge and development*, pages 17–42. Springer, 1977. 1
- [32] Joseph Redmon, Santosh Divvala, Ross Girshick, and Ali Farhadi. You only look once: Unified, real-time object detection. In *Proceedings of the IEEE conference on computer vision and pattern recognition*, pages 779–788, 2016. 1
- [33] Shaoqing Ren, Kaiming He, Ross Girshick, and Jian Sun. Faster r-cnn: Towards real-time object detection with region proposal networks. In *Advances in neural information pro*cessing systems, pages 91–99, 2015. 1
- [34] Karen Simonyan and Andrew Zisserman. Very deep convolutional networks for large-scale image recognition. arXiv preprint arXiv:1409.1556, 2014. 9
- [35] Alane Suhr, Mike Lewis, James Yeh, and Yoav Artzi. A corpus of natural language for visual reasoning. In *Proceedings of the 55th Annual Meeting of the Association for Computational Linguistics (Volume 2: Short Papers)*, pages 217–223, 2017. 1, 2
- [36] Alane Suhr, Stephanie Zhou, Ally Zhang, Iris Zhang, Huajun Bai, and Yoav Artzi. A corpus for reasoning about natural language grounded in photographs. In *Proceedings of the 57th Annual Meeting of the Association for Computational Linguistics*, pages 6418–6428, 2019. 1, 2
- [37] Alon Talmor, Jonathan Herzig, Nicholas Lourie, and Jonathan Berant. CommonsenseQA: A Question Answering Challenge Targeting Commonsense Knowledge. In Proceedings of the 2019 Conference of the North American Chapter of the Association for Computational Linguistics: Human Language Technologies, Volume 1 (Long and Short Papers),

- pages 4149-4158, 2019. 2
- [38] Peng Wang, Qi Wu, Chunhua Shen, Anthony Dick, and Anton van den Hengel. FVQA: Fact-based visual question answering. *IEEE transactions on pattern analysis and machine intelligence*, 40(10):2413–2427, 2018.
- [39] Xiaolong Wang, Ali Farhadi, and Abhinav Gupta. Actions transformations. In *Proceedings of the IEEE conference on Computer Vision and Pattern Recognition*, pages 2658–2667, 2016.
- [40] Ronald J Williams. Simple statistical gradient-following algorithms for connectionist reinforcement learning. *Machine learning*, 8(3-4):229–256, 1992.
- [41] R. J. Williams and D. Zipser. A learning algorithm for continually running fully recurrent neural networks. *Neural Computation*, 1(2):270–280, 1989. 6
- [42] Ning Xie, Farley Lai, Derek Doran, and Asim Kadav. Visual entailment task for visually-grounded language learning. arXiv preprint arXiv:1811.10582, 2018. 2
- [43] Ning Xie, Farley Lai, Derek Doran, and Asim Kadav. Visual entailment: A novel task for fine-grained image understanding. arXiv preprint arXiv:1901.06706, 2019. 2
- [44] Kexin Yi, Chuang Gan, Yunzhu Li, Pushmeet Kohli, Jiajun Wu, Antonio Torralba, and Joshua B. Tenenbaum. CLEVRER: Collision events for video representation and reasoning. In *International Conference on Learning Representations*, 2020. 2
- [45] Rowan Zellers, Yonatan Bisk, Ali Farhadi, and Yejin Choi. From Recognition to Cognition: Visual Commonsense Reasoning. In *The IEEE Conference on Computer Vision and Pattern Recognition (CVPR)*, June 2019. 1, 2
- [46] Peng Zhang, Yash Goyal, Douglas Summers-Stay, Dhruv Batra, and Devi Parikh. Yin and Yang: Balancing and answering binary visual questions. In *Conference on Computer Vision and Pattern Recognition (CVPR)*, 2016. 2
- [47] Yuke Zhu, Oliver Groth, Michael Bernstein, and Li Fei-Fei. Visual7w: Grounded question answering in images. In *Proceedings of the IEEE conference on computer vision and pattern recognition*, pages 4995–5004, 2016. 2
- [48] Tao Zhuo, Zhiyong Cheng, Peng Zhang, Yongkang Wong, and Mohan Kankanhalli. Explainable video action reasoning via prior knowledge and state transitions. In *Proceedings of the 27th ACM International Conference on Multimedia*, pages 521–529, 2019. 2